Catalysts **2015**, *5*, 1289-1303; doi:10.3390/catal5031289

OPEN ACCESS

catalysts

ISSN 2073-4344

www.mdpi.com/journal/catalysts

Article

Titanium-Niobium Oxides as Non-Noble Metal Cathodes for Polymer Electrolyte Fuel Cells

Akimitsu Ishihara [1,*], Yuko Tamura [2], Mitsuharu Chisaka [3], Yoshiro Ohgi [4], Yuji Kohno [2], Koichi Matsuzawa [2], Shigenori Mitsushima [1,2] and Ken-ichiro Ota [2]

[1] Institute of Advanced Sciences, Yokohama National University, 79-5 Tokiwadai, Hodogaya-ku, Yokohama 240-8501, Japan; E-Mail: mitsushi@ynu.ac.jp

[2] Green Hydrogen Research Center, Yokohama National University, 79-5 Tokiwadai, Hodogaya-ku, Yokohama 240-8501, Japan; E-Mails: tamura-yuko-zr@ynu.jp (Y.T.); kohnoy@ynu.ac.jp (Y.K.); kmatsu@ynu.ac.jp (K.M.); ken-ota@ynu.ac.jp (K.-i.O.)

[3] Department of Electronics and Information Technology, Hirosaki University, 3 Bunkyo-cho, Hirosaki, Aomori 036-8561, Japan; E-Mail: chisaka@eit.hirosaki-u.ac.jp

[4] Kumamoto Industrial Research Institute, 3-11-38 Azuma-cho, Azuma-ku, Kumamoto, Kumamoto 862-0901, Japan; E-Mail: ohgi@kumamoto-iri.jp

* Author to whom correspondence should be addressed; E-Mail: a-ishi@ynu.ac.jp; Tel.: +81-45-339-4021; Fax: +81-45-339-4024.

Academic Editor: Minhua Shao

Received: 2 June 2015 / Accepted: 14 July 2015 / Published: 17 July 2015

Abstract: In order to develop noble-metal- and carbon-free cathodes, titanium-niobium oxides were prepared as active materials for oxide-based cathodes and the factors affecting the oxygen reduction reaction (ORR) activity were evaluated. The high concentration sol-gel method was employed to prepare the precursor. Heat treatment in Ar containing 4% H_2 at 700–900 °C was effective for conferring ORR activity to the oxide. Notably, the onset potential for the ORR of the catalyst prepared at 700 °C was approximately 1.0 V *vs.* RHE, resulting in high quality active sites for the ORR. X-ray (diffraction and photoelectron spectroscopic) analyses and ionization potential measurements suggested that localized electronic energy levels were produced via heat treatment under reductive atmosphere. Adsorption of oxygen molecules on the oxide may be governed by the localized electronic energy levels produced by the valence changes induced by substitutional metal ions and/or oxygen vacancies.

Keywords: titanium-niobium oxides; oxygen reduction reaction; polymer electrolyte fuel cells; non-platinum cathode

1. Introduction

Polymer electrolyte fuel cells (PEFCs) offer many advantages, including high power density, high energy conversion efficiency, and lower operating temperatures. PEFCs are therefore suitable as power sources for vehicles and residential co-generation power systems. However, the use of Pt as a cathode electrocatalyst for PEFCs is problematic due to the high cost and limited availability of Pt, and insufficient stability of these catalysts. To successfully commercialize PEFCs, low-cost non-platinum cathode catalysts with high stability must be developed.

Since Jasinski discovered the oxygen reduction reaction (ORR) activity of cobalt phthalocyanine [1], the search for promising non-platinum ORR catalysts has led to the development of several cobalt- and iron-containing catalysts [2,3]. Approaches to enhance the activity of these catalysts include the use and optimization of carbon supports and heat treatment conditions. Heat treatment of iron salts adsorbed on carbon supports under ammonia gas is a recent breakthrough that produces catalysts with high ORR activities comparable to that of platinum-based catalysts [4]. Despite significant improvement of the ORR activity of non-platinum catalysts, issues regarding their long-term durability remain unresolved.

Based on the high stability of Group 4 and 5 metal oxide-based compounds in acidic media, low cost, [5,6] and lower solubility in acid solution compared to platinum-based catalysts, these compounds have piqued our interest as they are expected to be stable even under the conditions encountered at the PEFC cathode. Recently, we successfully synthesized oxide-based nanoparticles using oxy-metal phthalocyanines (MeOPc; Me = Ta, Zr, and Ti) as the starting material and multi-walled carbon nanotubes (MWCNTs) as the support as well as the electro-conductive material [7,8]. However, carbon materials are easily oxidized at high potentials with a consequent decrease of the ORR activity due to degradation of the electron conduction paths [8]. Thus, carbon-free electrocatalysts are required to achieve high durability of the oxide-based cathodes. To prepare noble-metal- and carbon-free cathodes, the basic approach is to combine electro-conductive oxides with oxides that possess ORR active sites.

Previously, we prepared noble-metal- and carbon-free cathodes comprising niobium-titanium oxides with active sites and titanium oxides with magneli phase Ti_4O_7 as the electro-conductive material (*i.e.*, $Ti_xNb_yO_z$ + Ti_4O_7) [9]. The highest onset potential of $Ti_xNb_yO_z$ + Ti_4O_7 was *ca.* 1.1 V *versus* the reversible hydrogen electrode (RHE). No degradation of the ORR performance of $Ti_xNb_yO_z$ + Ti_4O_7 was observed during the start-stop and load cycle tests in 0.1 mol·dm^{-3} H_2SO_4 at 80 °C, where these conditions are close to the operating conditions of the existing PEFC [10]. Therefore, we successfully demonstrated superior durability of noble-metal- and carbon-free oxide-based cathodes under the cathode conditions of the PEFC.

However, the ORR activities of the $Ti_xNb_yO_z$ + Ti_4O_7 catalysts were still low because these catalysts were prepared under argon containing 4% hydrogen at high temperature, 1050 °C, where Ti_4O_7 was

generated by the reduction of TiO_2. That is, the preparation conditions encouraged the formation of Ti_4O_7 but were not optimal for the formation of niobium-titanium oxides with active sites. Domen *et al.* demonstrated that Nb-doped TiO_2 synthesized by the oxidation of Nb-doped TiN nanoparticles exhibited definite ORR activity and high long-term stability in acidic solutions [11]. However, these catalysts contained carbon residues that functioned to improve the conductivity between the particle aggregates. The preparation conditions used in that study were thus not suitable for the formation of ORR active titanium-niobium oxides without carbon. Consequently, it is necessary to separately optimize the conditions for the formation of titanium-niobium oxides with active sites and the formation of electro-conductive oxides. In this study, we focus on the formation of active sites on titanium-niobium oxides using a high concentration sol-gel method. The factors that influence the ORR activity in the absence of a carbon support are evaluated. However, it is necessary to obtain sufficient electro-conductivity to evaluate the ORR activity of the titanium-niobium oxides. Even a glassy carbon (GC) rod is heat-treated in air, an insulating oxide film is not formed on the surface. Therefore, the GC rod is superior to use as a substrate for the working electrode. The present strategy utilizes pre-heat-treatment (600 °C in air for 10 min) to achieve sufficient electrical contact between the titanium-niobium oxides and the GC substrate. It is necessary to secure the sufficient electro-conductivity between oxide-based catalysts and conductive oxide support when carbon-free cathodes are prepared. For example, the electro-conductive oxide network is made preparations in advance. Then, after oxide-based precursor is supported on the network it is heat-treated to create the ORR active sites and to obtain sufficient electro-conductivity. In this study, the effects of the preparation conditions, such as the gas atmosphere and heat treatment temperatures, on the ORR activity of the titanium-niobium oxides employing a GC rod are evaluated.

2. Results and Discussion

2.1. Characterization of Catalysts

We prepared the titanium-niobium oxide samples with the charged total composition of $Ti_{0.841}Nb_{0.126}O_2$. Figure 1 shows the X-ray diffraction (XRD) patterns of the titanium-niobium oxide samples prepared at 600, 700, 800, 900, and 1050 °C (a) in air and (b) in Ar containing 4% H_2. The crystalline phase of the catalysts prepared by heat treatment in air at temperatures between 600 and 900 °C was identified as anatase TiO_2 (JCPDS no. 00-021-1272), indicating that the niobium atoms were incorporated into the TiO_2 anatase structure. According to phase diagram of TiO_2–Nb_2O_5 [12], Nb(V) ions dissolve into TiO_2 rutile structure only below *ca.* 10 atomic % in this temperature range. On the other hand, quasi-stable phase, TiO_2 anatase structure, can dissolve more Nb(V) ions. The phase transition from anatase to rutile occurred at temperatures above 900 °C. For samples prepared at higher temperatures, peaks corresponding to the rutile TiO_2 (JCPDS no. 00-021-1276) and $TiNb_2O_7$ (JCPDS no. 1001270) phases were observed. This is because the Nb(V) ions that cannot dissolve in the TiO_2 rutile structure forms complex oxides $TiNb_2O_7$ that is solid solution of TiO_2 and Nb_2O_5. Simultaneously, Nb-containing phases such as $TiNb_2O_7$ appeared at 1050 °C. These results are consistent with previous observations [13].

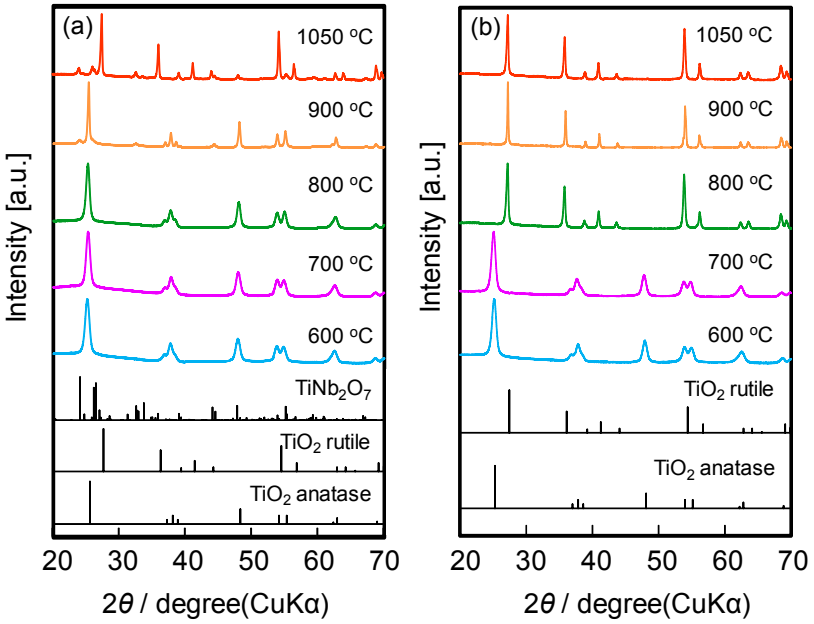

Figure 1. XRD patterns of titanium-niobium oxides prepared at 600, 700, 800, 900, and 1050 °C (**a**) in air and (**b**) in Ar containing 4% H_2.

The crystalline phase of the samples subjected to heat treatment at 600 and 700 °C in Ar containing 4% H_2 could be indexed to the TiO_2 anatase structure. However, the samples prepared at temperatures above 800 °C under this reductive atmosphere could be indexed to rutile TiO_2 with no Nb_2O_5 peaks. The shift of the XRD peaks to lower angles (Figure S1) with increasing treatment temperature suggested that the catalysts are substitutional solid solutions in which the niobium ions substitute titanium ions in the rutile TiO_2 lattice. Compared to formation of the rutile phase above 900 °C for the samples heat-treated in air, the rutile was phase formed at 800 °C under reductive atmosphere. Thus, the transformation from the anatase to rutile phase occurred at lower temperature under reductive atmosphere. In addition, the substitutional solid solution (rutile phase) was stable up to 1050 °C under reductive atmosphere. The XRD analysis clearly demonstrated that the TiO_2 rutile-based structure was more stable under reductive atmosphere than in air. This stabilization of the TiO_2 rutile-based structure is not predicted from the viewpoint of thermochemistry. The role of heat-treatment under reductive atmosphere and doped niobium ions must be elucidated.

Figures 2 and S2 show scanning electron microscopy (SEM) images of the titanium-niobium oxides prepared at 600 °C in air, and 600, 700, 800, 900, and 1050 °C in Ar containing 4% H_2. The SEM images demonstrate that the surface morphology of the titanium-niobium oxides depends on the heat treatment temperature. Very little difference in the surface morphology was observed for the samples prepared by heat treatment at 600 °C under different atmospheres. The particle size of the catalysts prepared at 600 °C was *ca.* several tens of nanometers. A significant change in the morphologies of the catalysts was observed with treatment at 800 °C, indicative of particle aggregation above 800 °C. Aggregation became progressive with increasing heat treatment temperatures. Thus, the surface area of the catalysts decreased with temperature, especially above 800 °C.

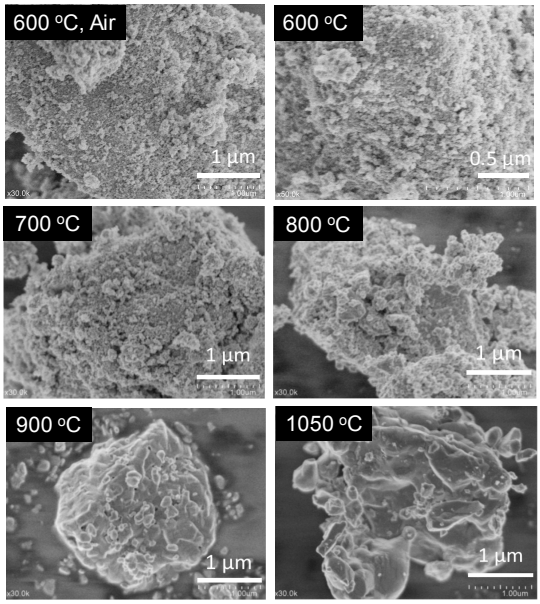

Figure 2. SEM images of the titanium-niobium oxides prepared at 600 °C in air, and 600, 700, 800, 900, and 1050 °C in Ar containing 4% H_2.

Figure 3 shows photographs of the catalysts prepared at 600 °C in air, and 600, 700, 800, 900, and 1050 °C in Ar containing 4% H_2. The powder heat-treated at 600 °C was white, as expected from the wide bandgap of TiO_2 (all samples treated in air were white). On the other hand, the samples heat-treated at 600 °C under reductive atmosphere had a light-blue color and the color deepened with increasing temperature. This color change suggests that there is some difference in the electronic energy levels of the samples prepared under reductive atmosphere relative to those prepared in air. Namely, the difference between the highest occupied and lowest unoccupied electronic energy levels decreases with increasing temperature. This color change suggests the development of a localized energy level of electrons in the bandgap of TiO_2.

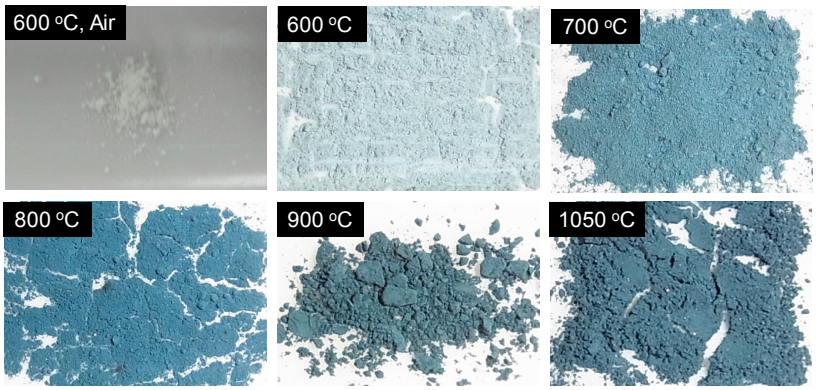

Figure 3. Photographs of the catalysts prepared at 600 °C in air, and 600, 700, 800, 900, and 1050 °C in Ar containing 4% H_2.

Figure 4a shows the Ti 2p XPS spectra of the catalysts prepared at 800 °C in air and in Ar containing 4% H_2. As anticipated, the Ti 2p XPS spectra revealed that Ti adopted the tetravalent state for the specimen heat-treated in air based on the $2p_{3/2}$ peak (TiO_2; 458.8 eV [14]). On the other hand, a low

valence state, *i.e.*, Ti^{3+} (Ti_2O_3; 456.8 eV [15]), was observed for the catalyst heat-treated at 800 °C under reductive atmosphere. The ratios of Ti^{3+}/Ti^{4+} calculated from areas of the XPS spectra of the specimens heat-treated at 800 °C in air and in Ar containing 4% H_2 were 5.0% and 10%, respectively. The ratio of the specimen prepared under reductive atmosphere was twice as large as that prepared in air. In addition, the total atomic ratio of Nb/Ti is 0.15 according to the charged total composition of $Ti_{0.841}Nb_{0.126}O_2$. The atomic ratios of Nb/Ti calculated from areas of the XPS spectra of the specimens heat-treated at 800 °C in air and in Ar containing 4% H_2 were 0.43 and 0.23, respectively. Both ratios are larger than the total atomic ratio, suggested that the niobium ions accumulate the surface of the oxide particles. In particular, the Nb/Ti ratio of the specimen heat-treated in air was about three times larger than the total atomic ratio. As mentioned in XRD patterns, because the rutile TiO_2 phase cannot dissolve the Nb(V) ions, the dissolved Nb(V) ions in the anatase TiO_2 phase began to accumulate near the surface of the particles at higher temperature heat treatment.

Figure 4b shows the Ti 2p XPS spectra of the catalysts prepared at 600, 700, 800, 900, and 1050 °C in Ar containing 4% H_2. Low valence states of Ti were observed for the catalyst heat-treated at 600 °C under reductive atmosphere, suggesting that the oxides underwent little reduction at 600 °C in Ar containing 4% H_2 upon treatment for 10 min. Heat-treatment above 700 °C under reductive atmosphere resulted in the formation of low valence state Ti as shown in Figure 4.

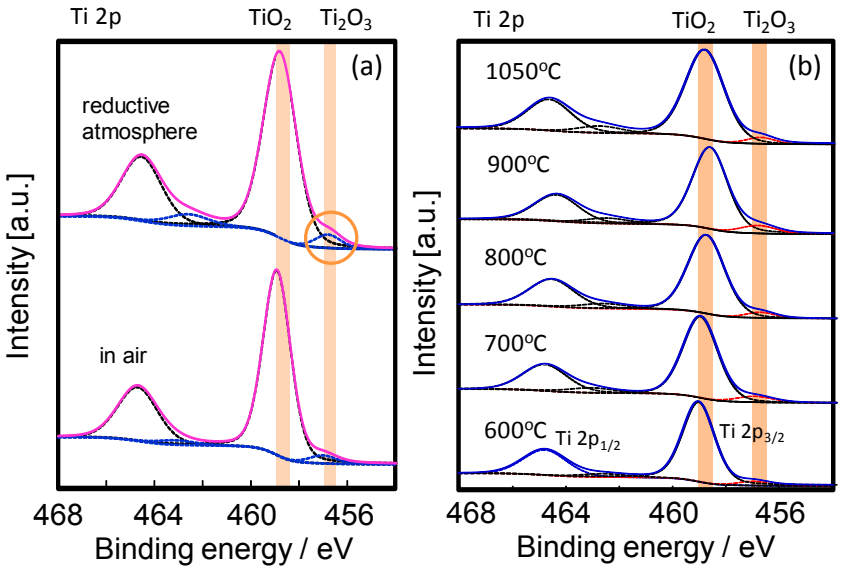

Figure 4. Ti 2p XPS spectra of the catalysts prepared at 800 °C in air and in Ar containing 4% H_2 (**a**) and prepared at 600, 700, 800, 900, and 1050 °C in Ar containing 4% H_2 (**b**).

Figure 5a shows the dependence of the ratios of Ti^{3+}/Ti^{4+} (expressed as $S_{Ti(III)}/S_{Ti(IV)}$) calculated from areas of the XPS spectra of the specimens heat-treated under reductive atmosphere on the temperature. The ratio of Ti^{3+}/Ti^{4+} of the specimen prepared at 600 °C is 6.7%. Ti^{3+} ions are produced by the substitution of the Nb^{5+} ions with Ti^{4+} ions of the TiO_2 lattice. Figure 5b shows the Nb 3d XPS spectra of the catalysts prepared at 600, 700, 800, 900, and 1050 °C in Ar containing 4% H_2. The peak in the Nb 3d spectra shifted to higher binding energy (NbO_2; 205.3 eV [16], Nb_2O_5; 207.1 eV [17]) with increasing heat treatment temperatures, in contrast with the Ti 2p peak. Therefore,

the Nb 3d XPS spectra revealed that most of Nb ions were highest oxidation state, 5+. Thus, the state of the specimens can be expressed as $Ti(IV)_{1-2x}Ti(III)_xNb(V)_xO_2$. If all Nb ions substitute Ti^{4+} ions of the TiO_2 lattice as Nb(V) ions, the composition is $Ti(IV)_{0.74}Ti(III)_{0.13}Nb(V)_{0.13}O_2$. Therefore, in that case, the ratio of Ti^{3+}/Ti^{4+} is calculated to be *ca.* 18%. The ratio of Ti^{3+}/Ti^{4+} at 600 °C, *ca.* 6.7%, was smaller than 18%, indicating that the Nb(V) ions did not sufficiently incorporate into the TiO_2 lattice at 600 °C. As shown in Figure 5a, the ratio of Ti^{3+}/Ti^{4+} increased with increasing temperature from 600 °C to 700 °C and saturated around 10%. These results deduced that reductive heat-treatment above 700 °C induced the formation of low valence state Ti.

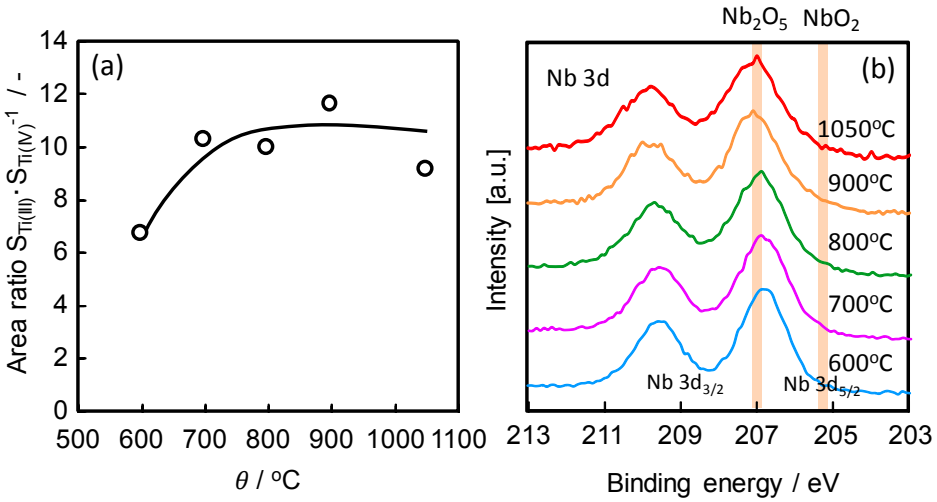

Figure 5. (**a**) Dependence of the ratios of Ti^{3+}/Ti^{4+}, $S_{Ti(III)}/S_{Ti(IV)}$, calculated from areas of the XPS spectra of the specimens heat-treated under reductive atmosphere on the temperature. (**b**) Nb 3d XPS spectra of the catalysts prepared at 600, 700, 800, 900, and 1050 °C in Ar containing 4% H_2.

Figure 6 shows the dependence of the atomic ratio of Nb/Ti calculated from XPS spectra of the specimens prepared under reductive atmosphere on the heat treatment temperature. The atomic ratio of Nb/Ti decreased with increasing temperature above 700 °C and approached the bulk value at 1050 °C. The XRD patterns revealed that the bulk phase transition occurred between 700 and 800 °C under reductive atmosphere. The XPS spectra indicated that the titanium ions near the surface were reduced and the Nb(V) ions near the surface incorporated into the TiO_2 lattice at *ca.* 700 °C. Therefore, the phase transition was probably caused by a change in the valence of titanium. We previously demonstrated that tantalum and zirconium oxide-based catalysts had some oxygen vacancies that acted as active sites for the ORR [6]. In case of the titanium-niobium oxide system, the low valence state of the metal ions does not always indicate the presence of oxygen vacancies. The low valence state of the metal ions can be achieved even in the absence of oxygen vacancies because the highest valence states of titanium and niobium are different. The relationship between the presence of oxygen vacancies and the active sites remains a topic for further study.

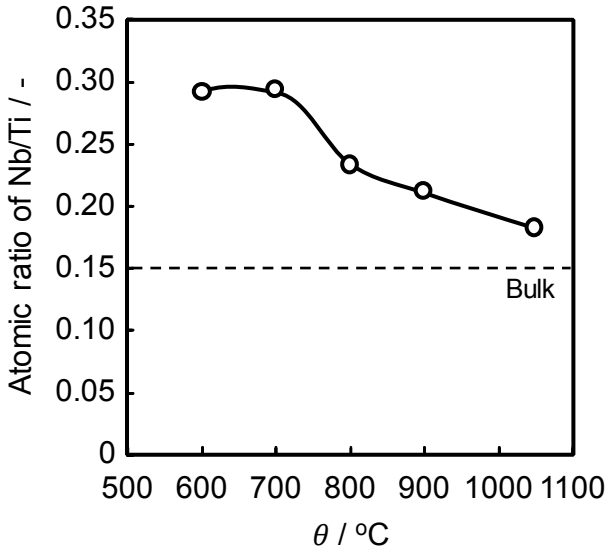

Figure 6. Dependence of the atomic ratio of Nb/Ti calculated from XPS spectra of the specimens prepared under reductive atmosphere on the heat treatment temperature.

It was difficult to evaluate the differences in the electronic state of the catalysts heat-treated under reductive atmosphere at temperatures between 700 and 1050 °C based on the XPS spectra, as shown in Figures 4b and 5a. Thus, the ionization potential of the specimens was used as a parameter to evaluate these differences. The ionization potentials of the specimens were measured using a photoelectron spectrometer surface analyzer in order to investigate the differences in the surfaces of the specimens heat-treated in reductive atmosphere at different temperatures. Figure 7a shows the relationship between the square root of the photoelectric quantum yield and the photon energy (that is, the photoelectron spectra of the specimens heat-treated at 800 °C in air or in Ar containing 4% H_2). The square root of the photoelectric quantum yield increased linearly with an increase in the photon energy applied to each specimen. The slope of the straight line reflects the tendency of the photoelectron emission of the specimens, that is, the density of state of the electrons near the Fermi level. Fewer photoelectrons were emitted in the case of the catalyst prepared in air. The slope of the straight line for the specimen heat-treated in air, where TiO_2 was identified on the sample surface by XPS, was apparently lower than that of the congener prepared under reductive atmosphere. It is remarkable that the slope of this plot was steeper for the specimen prepared in Ar containing 4% H_2. The intersection between the straight line and the background line in the photoelectron spectra provides the threshold energy corresponding to the photoelectric ionization potential. The photoelectric ionization potential corresponds to the highest energy level of the electrons in the materials. The ionization potential is directly affected by the localized electronic levels of the lattice defects and impurities in the metal oxides, such as valence changes due to substitutional metal ions, oxygen vacancies, and donor impurities.

Figure 7b shows the dependence of the ionization potential of the catalysts prepared at 600, 800, and 1050 °C in air, and 600, 700, 800, 900, and 1050 °C in Ar containing 4% H_2 on the heat treatment temperature, θ. The ionization potential of commercial rutile and anatase TiO_2 is 5.8 eV. The ionization potential was the same (*i.e.*, *ca.* 5.8 eV) for the catalysts prepared at 600, 800, and 1050 °C in air, suggesting that the surface of the catalysts prepared in air had few localized electronic levels from lattice defects and impurities in the metal oxides, similar to commercial TiO_2. On the other hand, the ionization potentials of the catalysts prepared under reductive atmosphere decreased with increasing temperature. The decrease in the ionization potential reflects an increase in the localized electronic levels. In other words, the valence changes due to substitutional metal ions, oxygen vacancies, and donor impurities increase with increasing temperature.

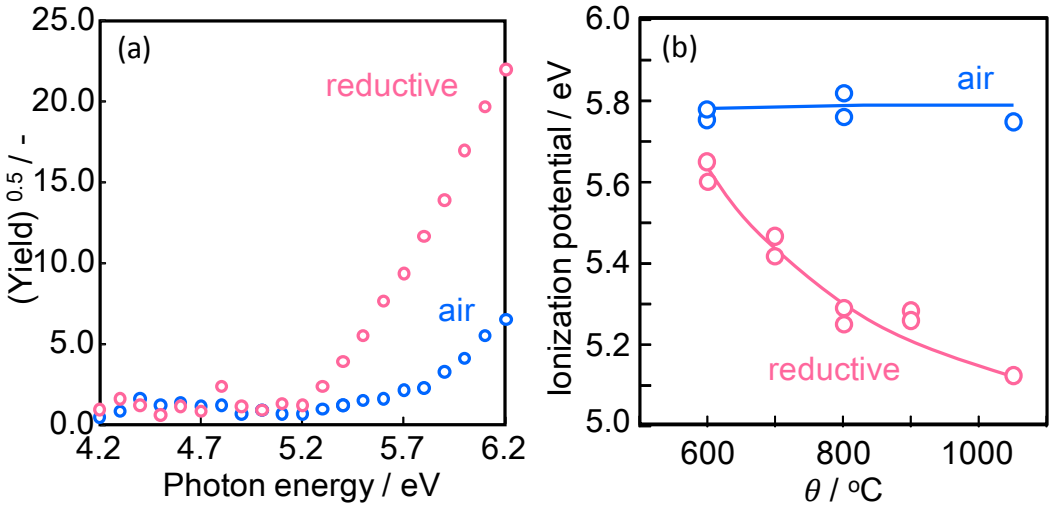

Figure 7. (**a**) Relationship between the square root of the photoelectric quantum yield ($Y^{1/2}$) and the photon energy of the specimens heat-treated at 800 °C in air or in Ar containing 4% H_2. (**b**) Dependence of the ionization potential of the catalysts prepared at 600, 800, and 1050 °C in air, and 600, 700, 800, 900, and 1050 °C in Ar containing 4% H_2 on the heat treatment temperature, θ.

2.2. Oxygen Reduction Activity in Acidic Media

Figure 8a shows the potential-i_{ORR} curves for the catalysts prepared at 600, 700, and 1050 °C in Ar containing 4% H_2. The heat treatment temperature apparently affected the ORR activity. We focused on the ORR activity in the higher potential region. Figure 8b shows the potential-i_{ORR} curves for the catalysts prepared at 600, 700, 800, 900, and 1050 °C in Ar containing 4% H_2. All samples prepared in air had a low ORR current in the potential range above 0.6 V, indicating that these catalysts have low ORR activity. On the other hand, although the ORR current was low, the catalysts prepared under reductive atmosphere exhibited some ORR activity. In particular, the onset potential of the ORR for the catalyst prepared at 700 °C was approximately 1.0 V *vs.* RHE. This high onset potential indicates the good suitability of the active sites for the ORR. Therefore, high quality active sites were created by heat treatment at 700 °C under reductive atmosphere.

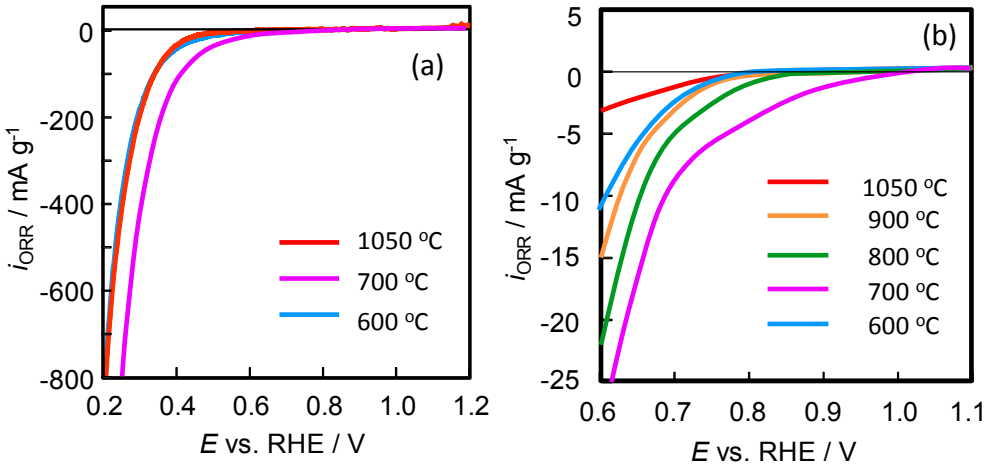

Figure 8. (**a**) Potential-i_{ORR} curves for the catalysts prepared 600, 700, and 1050 °C in Ar containing 4% H_2 and (**b**) potential-i_{ORR} curves in the higher potential region for the catalysts prepared 600, 700, 800, 900, and 1050 °C in Ar containing 4% H_2.

Figure 9 shows the dependence of the i_{ORR} @ 0.7 V on the heat-treatment temperature for the samples prepared under reductive atmosphere. The i_{ORR} @ 0.7 V reached a maximum around 700 °C. The i_{ORR} presented in Figure 9 is based on the mass of the catalysts loaded on the GC rod. As shown in Figures 2 and S2, the surface area of the catalysts declined precipitously above 800 °C. Thus, the decrease in the i_{ORR} @ 0.7 V above 800 °C seems to be due to the decrease in the surface area. To evaluate the specific activity (*i.e.*, the ORR current density based on surface area) the actual surface area of the oxides must be estimated. However, it is difficult to estimate the surface area of the oxides because neither hydrogen nor CO is adsorbed by the oxides. Therefore, the electrical charges of the double layer of the catalysts calculated from the cyclic voltammogram (CV) in N_2 atmosphere were used to evaluate the apparent specific activity of the catalysts. Figure S3 shows the cyclic voltammograms of the GC rod only and of titanium-niobium oxide supported on the GC rod ($Ti_xNb_yO_z$/GC) heat-treated at 800 °C under reductive atmosphere. Because the amount of oxide catalyst loaded on the rod was small (*ca.* 1 mg), the charge/discharge current was mainly derived from that due to the GC substrate. The electrical charge due to the oxide was estimated from the difference between the CV of $Ti_xNb_yO_z$/GC and that of GC only. Figure S4 shows the dependence of the electrical charge of the double layer of the oxides on the catalyst loading. The SEM images showed that the surface area of the catalysts decreased above 800 °C due to aggregation of the particles. However, a linear relationship was obtained, suggesting that the electrical charge was determined not by the heat treatment temperature but by the catalyst loading. Therefore, the trend in the apparent specific activity (ORR current density based on electrical charge) is similar to that of the mass activity. It is anomalous that the electrical charge is independent of the heat treatment temperature. The surface area estimated using the electrical charge may be different from that predicted from the SEM images. Because the electrical conductivity of even the catalysts prepared under reductive atmosphere is low, the surface area of the electrochemical active region in contact with the GC rod might be small. Thus, a more accurate estimation of the actual surface area of the catalysts is necessary.

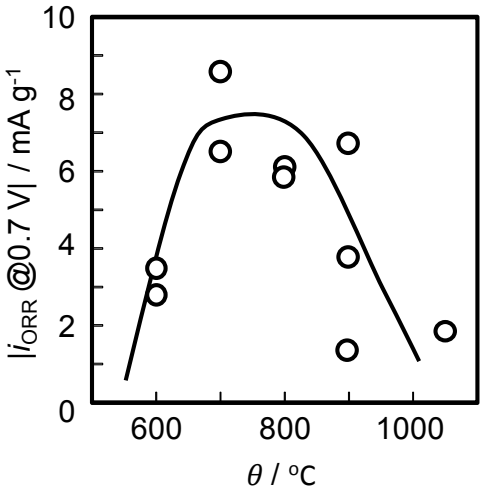

Figure 9. Dependence of i_{ORR} @ 0.7 V on temperature used for heat-treatment of the samples under reductive atmosphere.

2.3. Relationship between ORR Activity and Physico-Chemical Properties

The ORR activity was enhanced by reductive heat treatment in the region of 700 to 900 °C. The XRD patterns indicated that the crystalline structure of the catalysts prepared under reductive atmosphere changed from anatase to rutile TiO_2 around 800 °C. On the other hand, the XPS spectra revealed that low valence state Ti is generated by heat treatment above 700 °C under reductive atmosphere. Therefore, reduction of the sample surface occurs around 700 °C. The ionization potential is more sensitive to the surface state as shown in Figure 7b. Henrich *et al.* found that the work function (*i.e.*, ionization potential in this study) of TiO_2 decreased as the density of oxygen vacancies increased [18]. Therefore, the low ionization potential suggested that the catalysts heat-treated under reductive atmosphere at higher temperature had more surface defects. In this study, the oxygen vacancies as well as the valence changes induced by substitutional metal ions were found to produce localized electronic energy levels in the bandgap.

Figure 10 shows the relationship between the ionization potential and the i_{ORR} @ 0.7 V of the catalysts prepared under reductive atmosphere. A "volcano plot" with a maximum at 5.4 eV was obtained, suggesting that the electronic state of the sample surface is suitable for the ORR.

Adsorption of oxygen molecules on the surface is required as the first step for the ORR to proceed. Many studies have demonstrated that surface defect sites are required for adsorption of oxygen molecules on the surface of the oxides [19]. Therefore, a larger number of surface defects furnishes more sites for adsorption of oxygen molecules. In addition, the interaction of oxygen with the catalyst surface is essential because adsorption of oxygen and desorption of water from the surface are both necessary for robust progress of the ORR. When the interaction of oxygen with the catalyst surface is strong, desorption of water does not proceed readily. On the other hand, when the interaction of oxygen with the catalyst surface is weak, less adsorption of oxygen molecules occurs. Therefore, there is an optimal strength for the interaction between oxygen and the catalyst surface. Metallic Ti adsorbs oxygen strongly because of the large adsorption energy of oxygen (759 $kJ \cdot mol^{-1}$) and the strong energy of the Ti-oxygen bonds (calculated: 625 $kJ \cdot mol^{-1}$) [20]. In the case of Pt, the energy for adsorption of oxygen and the calculated Pt-oxygen bond energy are 272 $kJ \cdot mol^{-1}$ and 385 $kJ \cdot mol^{-1}$, respectively [20]. Therefore,

the corresponding values for Ti are much larger than those of Pt. As the degree of oxidization of metallic Ti increases, the interaction of oxygen with Ti on the catalyst surface is weakened because the oxide ions attract the electrons in the highest occupied molecular orbital of Ti thereby conferring a positive charge on Ti, *i.e.*, higher valence state. Because the ionization potential is related to the strength of the interaction between the surface of the specimen and oxygen, the volcano plot shown in Figure 10 suggests that there is a suitable interaction between the surface of the specimen and oxygen. Consequently, the strength of the interaction between oxygen and the oxide surface could be manipulated by controlling the local energy level of the electrons, *i.e.*, by controlling the valence changes induced by the substitutional ions and/or oxygen vacancies.

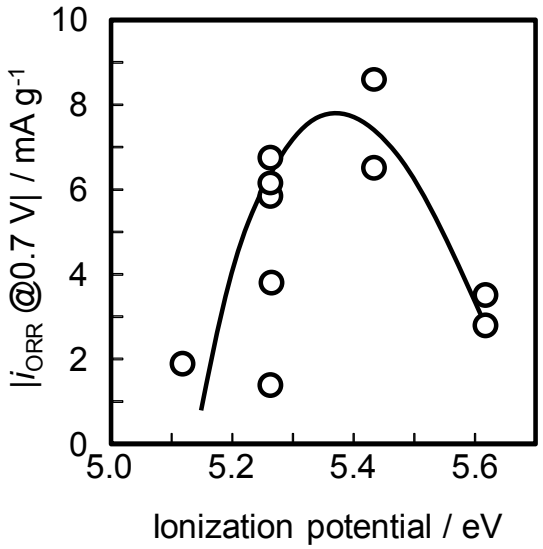

Figure 10. Relationship between the ionization potential and the i_{ORR} @ 0.7 V of the catalysts prepared under reductive atmosphere.

3. Experimental Section

The high concentration sol-gel method [21,22] was used for preparation of the precursor. A 30 cm^3 aliquot of titanium(IV) tetraisopropoxide ($C_{12}H_{28}O_4Ti$, 99.99%, Sigma-Aldrich Japan Co. LLC, Tokyo, Japan) and 4 cm^3 of niobium(V) ethoxide ($C_{10}H_{25}NbO_5$, 99.95%, Aldrich) were dissolved in 200 cm^3 of 2-methoxyethanol with a TiO_2:Nb_2O_5 weight ratio of 8:2. The mixed solution was maintained at −50 °C, and 15 cm^3 of 2-methoxyethanol in 15 cm^3 of pure water was added to the mixed solution dropwise. The temperature of the solution was raised to 80 °C and maintained for 3 weeks as an aging treatment, resulting in the formation of nano-sized complex oxides. The precipitates were dispersed in 2-methoxyethanol to obtain a dispersion of nano-sized titanium-niobium oxide.

A 3-mm^3 aliquot of the dispersion was dropped onto a GC rod (φ = 5.0 mm; TOKAI CARBON CO., LTD., Tokyo, Japan) followed by drying at room temperature. The coated rod was heat-treated at 600 °C for 10 min in air as a pre-heat-treatment step to remove organic species and carbon residue and to provide sufficient electrical contact between the titanium-niobium oxide and the GC substrate. Subsequently, samples of titanium-niobium oxide supported on the GC rods were heat-treated at 600, 700, 800, 900, and 1050 °C in air or in Ar containing 4% H_2 to prepare the working electrodes. For the powder XRD and ionization potential measurements, 3 cm^3 of the dispersion of nano-sized

titanium-niobium oxide was dried on a hot plate at 160 °C to obtain the powder samples. The powders were then heat-treated at 600 °C for 10 min in air to remove organic species and carbon residue. The powders were subsequently heat-treated at 600, 700, 800, 900, or 1050 °C in air or in Ar containing 4% H_2 for powder XRD and ionization potential measurements.

The morphologies, crystalline structures, and chemical states of the synthesized catalysts were investigated by transmission electron microscopy (TEM; JEOL Ltd., JEM-2100F, Akishima, Japan, X-ray diffraction (XRD; Rigaku Corporation, Ultima IV, X-ray source: Cu-Kα, Akishima, Japan) and X-ray photoelectron spectroscopy (XPS; ULVAC-PHI, Inc. Quantum-2000, X-ray source: monochromated Al-Kα radiation, Chigasaki, Japan). The peak of the C–C bond attributed to free carbon at 284.6 eV in the C 1s spectrum was used to compensate for surface charging.

The ionization potential of the specimens was measured using a photoelectron spectrometer surface analyzer (Model AC-2, RIKEN KEIKI Co., Ltd., Tokyo, Japan) [23,24].

All electrochemical measurements were performed in 0.1 $mol \cdot dm^{-3}$ H_2SO_4 at 30 °C with a 3-electrode cell. A reversible hydrogen electrode (RHE) and a glassy carbon plate were used as the reference and counter electrodes, respectively. As a pre-treatment, 300 CV cycles were performed in O_2 atmosphere in the range of 0.05 to 1.2 V with respect to the RHE at a scan rate of 150 $mV \cdot s^{-1}$. Slow scan voltammetry was performed under O_2 and N_2 atmosphere in the range of 0.2 to 1.2 V with respect to RHE at a scan rate of 5 $mV \cdot s^{-1}$. The ORR current density, i_{ORR}, based on the mass of the catalyst (mass activity), was determined by calculating the difference between the current density under O_2 and N_2 atmosphere.

4. Conclusions

In order to develop noble-metal- and carbon-free cathodes, titanium-niobium oxides were prepared for use as oxide-based cathodes and the factors affecting the ORR activity and active sites were evaluated. The high concentration sol-gel method was employed for preparation of the precursor. Secure adhesion between the oxide catalysts and the substrate was achieved by heating the precursor supported GC rod at 600 °C in air to maintain the electrical contact as a pretreatment step. To create ORR active sites, the precursor supported GC rod was heat-treated in the temperature range of 600 to 1050 °C in air or in Ar containing 4% H_2. Heat treatment in reductive atmosphere at 700–900 °C was effective for conferring ORR activity to the catalysts. Notably, the onset potential for the ORR was approximately 1.0 V *vs.* RHE for the catalyst prepared at 700 °C. This high onset potential indicates the high quality of the active sites for the ORR. XRD, XPS and ionization potential measurements suggested that localized electronic energy levels were produced by heat treatment under reductive atmosphere. The electronic energy levels produced by the valence changes of Ti induced by substitutional metal ions and/or oxygen vacancies might govern adsorption of the oxygen molecules. Therefore, the strength of the interaction between oxygen and the oxide surface can be manipulated by controlling the valence changes induced by the substitutional ions and/or oxygen vacancies.

Acknowledgments

The authors acknowledge financial support from the New Energy and Industrial Technology Development Organization (NEDO). This work was conducted under the auspices of the Ministry of

Education, Culture, Sports, Science and Technology (MEXT) Program for Promoting the Reform of National Universities.

Author Contributions

A.I. designed the research; Y.T. performed research; M. C. analyzed XPS data; Y.O. analyzed data; and all authors provided feedback during preparation of the manuscript.

Conflicts of Interest

The authors declare no conflict of interest.

References

1. Jasinski, R. A new fuel cell cathode catalyst. *Nature* **1964**, *201*, 1212–1213.
2. Jaouen, F.; Goellner, V.; Lefevre, M.; Herranz, J.; Proietti, E.; Dodelet, J.P. Oxygen reduction activities compared in rotating-disk electrode and proton exchange membrane fuel cells for highly active Fe–N–C catalysts. *Electrochim. Acta* **2013**, *87*, 619–628.
3. Wu, G.; More, K.L.; Johnston, C.M.; Zelenay, P. High-Performance Electrocatalysts for Oxygen Reduction Derived from Polyaniline, Iron, and Cobalt. *Science* **2011**, *332*, 443–447.
4. Proietti, E.; Jaouen, F.; Lefevre, M.; Larouche, N.; Tian, J.; Herranz, J.; Dodelet, J.P. Iron-based cathode catalyst with enhanced power density in polymer electrolyte membrane fuel cells. *Nat. Commun.* **2011**, *2*, 416.
5. Ishihara, A.; Lee, K.; Doi, S.; Mitsushima, S.; Kamiya, N.; Hara, M.; Domen, K.; Fukuda, K.; Ota, K. Tantalum Oxynitride for a Novel Cathode of PEFC. *Electrochem. Solid-State Lett.* **2005**, *8*, A201–A203.
6. Ishihara, A.; Tamura, M.; Ohgi, Y.; Matsumoto, M.; Matsuzawa, K.; Mitsushima, S.; Imai, H.; Ota, K. Emergence of Oxygen Reduction Activity in Partially Oxidized Tantalum Carbonitrides: Roles of Deposited Carbon for Oxygen-Reduction-Reaction-Site Creation and Surface Electron Conduction. *J. Phys. Chem. C* **2013**, *117*, 18837–18844.
7. Ishihara, A.; Chisaka, M.; Ohgi, Y.; Matsuzawa, K.; Mitsushima, S.; Ota, K. Synthesis of nano-TaO_x oxygen reduction reaction catalysts on multi-walled carbon nanotubes connected via a decomposition of oxy-tantalum phthalocyanine. *Phys. Chem. Chem. Phys.* **2015**, *17*, 7643–7647.
8. Okada, Y.; Ishihara, A.; Matsumoto, M.; Imai, H.; Kohno, Y.; Matsuzawa, K.; Mitsushima, S.; Ota, K. Electrochemical stability of zirconium oxide-based electrocatalysts made from oxy-zirconium phthalocyanines. *J. Electrochem. Soc.* **2015**, *162*, F959–F964.
9. Ishihara, A.; Hamazaki, M.; Kohno, Y.; Matsuzawa, K.; Mitsushima, S.; Ota, K. Titanium-niobium oxides mixed with Ti_4O_7 as noble-metal- and carbon-free cathodes for polymer electrolyte fuel cells. *Electrochim. Acta*, submitted.
10. Hamazaki, M.; Ishihara, A.; Kohno, Y.; Matsuzawa, K.; Mitsushima, S.; Ota, K. Evaluation of durability of titanium-niobium oxides mixed with Ti_4O_7 as non-noble and carbon-free cathodes for PEFC in H_2SO_4 at 80 °C. *Electrochemistry*, in press.

11. Arashi, T.; Seo, J.; Takanabe, K.; Kubota, J.; Domen, K. Nb-doped TiO_2 cathode catalysts for oxygen reduction of polymer electrolyte fuel cells. *Catal. Today* **2014**, *233*, 181–186.
12. The American Ceramic Society. *In Phase Equilibria Diagrams Volume XII Oxides*; McHale, A., Roth, R., Gen, S., Eds.; The American Ceramic Society, United States of America: Westerville, OH, USA, 1996; p. 119.
13. Sedneva, T.A.; Lokshin, E.P.; Belikov, M.L.; Belyaevskii, A.T. TiO_2-and Nb_2O_5-Based Photocatalytic Composites. *Inorg. Mater*. **2013**, *49*, 382–389.
14. Haukka, S.; Lakomaa, E.-L.; Jylha, O.; Vilhunen, J.; Hornytzkyj, S. Dispersion and Distribution of Titanium Species Bound to Silica from $TiCl_4$. *Langmuir* **1993**, *9*, 3497–3506.
15. González-Elipe, A.R.; Munuera, G.; Espinos, J.P.; Sanz, J.M. Compositional changes induced by 3.5 keV Ar^+ ion bombardment in Ni–Ti oxide systems: A comparative study. *Surf. Sci.* **1989**, *220*, 368–380.
16. Bahr, M.K. ESCA studies of some niobium compounds. *J. Phys. Chem. Solids* **1975**, *36*, 485–491.
17. Olejniczak, M.; Ziolek, M. Comparative study of Zr, Nb, Mo containing SBA-15 grafted with amino-organosilanes. *Microporous Mesoporous Mater.* **2014**, *196*, 243–253.
18. Henrich, V.E.; Dresselhaus, G.; Zeiger, H.J. Observation of Two-Dimensional Phases Associated with Defect States on the Surface of TiO_2. *Phys. Rev. Lett.* **1976**, *36*, 1335–1339.
19. Bourgeois, S.; Domenichini, B.; Jupille, J. Excess Electrons at Oxide Surfaces. In *Defects at Oxide Surfaces*; Jupille, J., Thornton, G., Eds.; Springer Series in Surface Sciences 58; Springer International Publishing: Basel, Switzerland, 2015; pp. 123–148.
20. Miyazaki, E.; Yasumori, I. Heats of chemisorption of gases. *Surf. Sci.* **1976**, *55*, 747–753.
21. Matsuda, H.; Mizushima, T.; Kuwabara, M. Low-Temperature Synthesis and Electrical Properties of Semiconducting $BaTiO_3$ Ceramics by the Sol-Gel Method with High Concentration Alkoxide Solutions. *J. Ceram. Soc. Jpn.* **1999**, *107*, 290–292.
22. Matsuda, H.; Kobayashi, N.; Kobayashi, T.; Miyazawa, K.; Kuwabara, M. Room-temperature synthesis of crystalline barium titanate thin films by high-concentration sol-gel method. *J. Non-Cryst. Solids* **2000**, *271*, 162–166.
23. Kirihata, H.; Uda, M. Externally quenched air counter for low-energy electron emission measurements. *Rev. Sci. Instrum.* **1981**, *52*, 68–70.
24. Uda, M.; Nakagawa, Y.; Yamamoto, T.; Kawasaki, M.; Nakamura, A.; Saito, T.; Hirose, K. Successive change in work function of Al exposed to air. *J. Electron. Spectrosc. Relat. Phenom.* **1998**, *88–91*, 767–771.